Desalination and Water Treatment
www.deswater.com
doi: 10.1080/19443994.2016.1146919

57 (2016) 24970–24981
November

Taylor & Francis
Taylor & Francis Group

Removal of quinclorac herbicide from aqueous solution by chitosan/montmorillonite bionanocomposite

Chunxia Ding[a,b], Daoxin Gong[b,c,*], Peng Yu[a], Jihai Shao[c], Mei-E Zhong[a]

[a]*College of Science, Hunan Agricultural University, Changsha 410128, P.R. China, emails: dcxxcn@163.com (C. Ding), yuzhiyipeng@163.com (P. Yu), xiaomei9902@126.com (M.-E. Zhong)*
[b]*Institute of Tobacco Research, Hunan Agricultural University, Changsha 410128, P.R. China, Tel. +86 731 84617710; email: gdx0745@163.com (D. Gong)*
[c]*College of Resource and Environment, Hunan Agricultural University, Changsha 410128, P.R. China, email: shaojihai@gmail.com (J. Shao)*

Received 7 February 2015; Accepted 19 January 2016

ABSTRACT

Chitosan–montmorillonite bionanocomposite (CTS–MMT) was prepared for removing the herbicide quinclorac (QC) from aqueous solution. The resulting nanocomposites were characterized by X-ray powder diffraction (XRD), Fourier transform infrared spectroscopy (FTIR), scanning electron microscopy (SEM), Brunauer–Emmett–Teller (BET) surface area and Barrett–Joyner–Halenda (BJH) pore size distribution analysis. The adsorption of QC onto CTS–MMT as a function of adsorbent dosage, pH, temperature, ionic strength, contact time, and initial QC concentration was investigated by conducting batch adsorption experiments. The results showed that CTS–MMT exhibited higher adsorption affinity and higher adsorption capacity towards QC than the unmodified montmorillonite. The adsorption kinetics data of QC onto CTS–MMT were well described by the pseudo-second-order kinetics model. Adsorption isotherms fitted well with the Freundlich isotherm model in the heterogeneous adsorption process. Adsorption thermodynamics study indicated that the adsorption of QC onto CTS–MMT was a spontaneous and endothermic process. The QC molecules on CTS–MMT could hardly be desorbed by water, but could be desorbed by 0.1 mol/L NaOH solution. QC adsorption on CTS–MMT may involve electrostatic attraction, cation–dipole, hydrogen bonding, and van der Waals interactions. The findings of this study suggest that CTS–MMT is a potential adsorbent for quinclorac pollution remediation.

Keywords: Quinclorac; Herbicide; Chitosan; Montmorillonite; Adsorption

1. Introduction

Quinclorac (3,7-dichloroquinoline-8-carboxylic acid) is a highly selective herbicide which is widely used in rice crops in many countries, such as in Brazil, United States, Uruguay, China, etc. [1,2]. However, it has been reported that quinclorac has adverse effects on aquatic animals and hydrophytes. Besides, it is considered to be a hepatic and renal toxicant because of its characteristics of persistence, high toxicity, and bioaccumulation [3,4]. Furthermore, its residues in soil may cause potential hazards to rotate crops and ecological environment [5,6]. It is reported that due to its high mobility, quinclorac contamination spreads

*Corresponding author.

from rice production areas to nearby aquatic systems through various pathways [7–10]. In recent years, many studies reveal that quinclorac is a common agrochemical residue in the waters near paddy fields, and it has been the most frequently detected agrochemical residue in some countries [11,12]. Therefore, it is very important to explore viable remediation methods for quinclorac-polluted waters.

Some methods for removing quinclorac have been proposed, including photolytic and photocatalytic degradation [2,12], biodegradation [13], and adsorption [10,14]. Among these methodologies, adsorption has been found to be one of the most popular, efficient, and cheapest methods for removing quinclorac from aqueous solution [14]. In recent years, new practices have been focused on the use of clay minerals as an alternative to the conventional adsorbents, based on their advantages of low cost and nontoxicity [15]. Among many kinds of clay minerals, montmorillonite is the most commonly used adsorbent for removing heavy metal ions [16] and organic contaminants [17–20], due to its large specific surface area and cation-exchange capacity. However, the montmorillonite clay has low affinity to negatively charged or neutral contaminants because of the hydrophilic nature of its surfaces, resulting from the hydration of exchangeable cations and the isomorphic substitutions [21]. In order to improve its adsorption capacity for neutral or negatively charged contaminants, montmorillonites have been treated with some organic reagents, such as ammonium acetate [22], stearyl dimethylbenzyl ammonium cations [23], octadecyltrimetylammonium bromide [24], hexadecylpyridinium, dihexadecyldimetylammonium [25], poly (4-vinylpyridine-co-styrene), and polydiallyldimethylammonium chloride [26–28]. However, these organic modifiers may cause secondary pollution.

In order to reduce such secondary pollution, some natural organic cations have also been used as modifiers [29]. Natural polymeric materials have attracted wide attention for application as adsorbents in wastewater treatment due to their characteristics of nontoxic, biodegradable nature, and biocompatibility [30]. Chitosan is a natural polyaminosaccharide polymer synthesized from the deacetylation of chitin, which is the second most plentiful natural polymer after cellulose [31]. As a well-known adsorbent, chitosan has been widely used for the removal of transition metal ions and organic contaminants due to the presence of amino ($–NH_2$) and hydroxyl (–OH) groups, which can serve as active adsorption sites [32–35]. Nevertheless, the application of chitosan sometimes has been limited due to its low specific gravity, weak mechanical strength and solubility in acidic solutions [36,37]. Moreover, pure chitosan tends to agglomerate and form a gel in aqueous solution, making most of the active groups inaccessible for metal ions and organic contaminants binding [38]. Coating chitosan as a thin layer onto montmorillonite will increase the accessibility of its binding sites and improve its mechanical performance and adsorption capacity [39–41]. Darder et al., firstly prepared and characterized chitosan-clay nanocomposites [42]. Celis et al., found that chitosan–montmorillonite can be useful as adsorbents for the removal of anionic clopyralid herbicide [43]. Nevertheless, no study has been hitherto conducted to investigate the removal of quinclorac using the montmorillonite modified by chitosan.

In this study, the natural montmorillonite (MMT) was firstly treated with 1.0 mol/L NaCl, and then the Na^+-treated montmorillonite (named as NaMMT) was modified by chitosan at different loadings. The adsorption capacities of quinclorac onto the as-made CTS–MMTS were compared and the optimum adsorbent (CTS–MMT) was applied to removing quinclorac from water. The materials were characterized by XRD, FTIR, SEM, BET, and BJH analysis. The effects of various parameters on quinclorac adsorption were investigated to verify the actual results of modification. Batch experiments were carried out to determine the adsorption kinetics and isotherms of quinclorac, and the adsorption mechanisms of quinclorac onto CTS–MMT were also proposed.

2. Materials and methods

2.1. Materials

The natural montmorillonite (the cation-exchange capacity is 87 mmol/100 g) was obtained from Zhejiang Anji Rongjian Mineral Refining Factory, Zhejiang of China. Chitosan (molecular weight, MW = 1,000,000 g/mol, degree of deacetylation, DD = 80%) was purchased from Aladdin Industrial Inc., Shanghai, China. Quinclorac (with purity 98.1%, MW = 242.06) was supplied by Institute for the Control of Agrochemicals, Pekin, China. Quinclorac's solubility in water is 49 mg/L, and the value of pK_a for quinclorac is 4.3 [44]. The structure of quinclorac is shown in Fig. 1. All other inorganic chemicals of analytical grade were purchased from Sinopharm Group Chemical Reagent Limited Company, China.

2.2. Modification of MMT with different mass ratios of chitosan

The NaMMT was prepared by treating natural montmorillonite with 1.0 mol/L NaCl. The natural

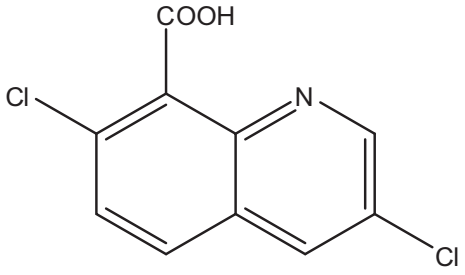

Fig. 1. Molecular structure of quinclorac.

montmorillonite (6 g) was mixed with 200 mL of 1.0 mol/L NaCl and the mixture was stirred magnetically for 24 h [42,45]. The resultant suspension was filtrated and then washed with distilled water until no precipitate was observed in the filtrate, confirmed by the $AgNO_3$ test. Finally, the obtained NaMMT was dried at 100˚C for 24 h.

CTS–MMT was prepared using the following method. CTS of corresponding amounts (0, 0.2, 0.4, 0.6, 0.8, 1.0, 1.2, 1.4, 1.6, 1.8, 2.0 g, respectively.) was dissolved in 200 mL 0.05% HCl solution, and the mixed solution was stirred for 4 h, with its pH adjusted to 5.0 with 0.1 M NaOH. Then, 1.0 g NaMMT was added to the dissolved CTS solution, and the resultant mixture was stirred for 5 h. The suspension was filtrated, and washed with distilled water to remove chloride ions, sodium ions, and excess chitosan. The composite was dried at 60˚C for 24 h. After drying up, the materials were ground to powder.

2.3. Materials characterization

Fourier transform infrared (FTIR) spectra of the samples were characterized on an IRAffinity-1 FTIR spectrometer (SHIMADZU, Japan) using KBr pressing method. X-ray diffraction (XRD) analyses of the powder samples were performed on an XRD-6000 X-ray diffractometer (SHIMADZU, Japan) with Cu Kα radiation ($\lambda = 0.15406$ nm), running at 40 kV and 30 mA, scanning from 2˚ to 30˚ at 2˚/min. The micrographs of the samples were obtained using JSM-6380LV scanning electron microscopy (SEM) (JEOL, Japan). The surface area and pore size of the samples were determined by nitrogen adsorption–desorption using a Quadrasorb SI analyzer (Quantachrome, USA). The pH zero point of charge (pH_{pzc}) of CTS–MMT was determinated according to the method used by Zhou et al. [46]. Elemental analyses were performed in a CE-440 elemental analyzer (EAI, USA).

2.4. Adsorption experiments

2.4.1. Comparison of adsorption percentage of QC onto the CTS–MMTs

The influence of the mass ratio difference of chitosan and NaMMT on QC adsorption was studied at about pH 5.2 using 40-mL centrifuge tubes lined with screw caps. The initial concentration of QC was set at 10 mg/L, the volume of QC solution was 10.0 mL, and the adsorbent dosage was 50 mg. The optimum adsorbent (CTS–MMT) was used in the following experiments.

2.4.2. Batch adsorption studies

The batch adsorption experiments were carried out to evaluate QC adsorption equilibrium time and adsorption kinetics onto CTS-MMT. 50 mg of CTS–MMT was added into 10 mL QC solution with an initial concentration of 10 mg/L. The centrifuge tubes were placed in a constant temperature shaker with 150 rpm at 25˚C. The suspensions were sampled at different time intervals, centrifuged (4,000 rpm, 10 min), and then analyzed using high-performance liquid chromatography (HPLC). The amount of adsorbed QC (q_t, mg/g) can be calculated according to Eq. (1):

$$q_t = \frac{(C_0 - C_t)V}{m} \tag{1}$$

where C_0 and C_t are the initial and final aqueous phase concentrations of the QC, respectively (mg/L). V is the volume of the QC solution (L), and m is the dosage of the adsorbent (g). The adsorption percentage of QC was calculated according to Eq. (2):

$$\text{Adsorption percentage } (\%) = \frac{C_0 - C_t}{C_0} \times 100 \tag{2}$$

For the adsorption isotherm test, 50 mg of CTS–MMT was added into 10 mL of QC solution with initial concentrations varying from 1 to 30 mg/L. The temperature was set at 298, 308, and 318 K, respectively.

The effect of pH on QC adsorption was investigated in a pH range from 2.90 to 10.32, which was adjusted by adding 0.1 mol/L NaOH or 0.1 mol/L HCl solutions. A series of tubes containing 50 mg of CTS–MMT and 10 mL of 10 mg/L QC solution with different pHs were shaken for 24 h. The influence of adsorbent dosage on QC adsorption was observed when the dosage of CTS–MMT varied from 10 to

200 mg. Ionic strength test was conducted by adding 50 mg of CTS–MMT into 10 mL of NaCl (0–0.1 mol/L) solution containing 10 mg/L QC.

2.5. Desorption experiments

Desorption experiments were conducted immediately after adsorption equilibrium. About 5.0 mL of supernatant solution removed for the adsorption analysis was replaced with 5.0 mL of either water or 0.1 M NaOH. After shaking at 25°C for 24 h, the mixture was centrifuged, and then 5.0 mL of supernatant were removed, filtered, and analyzed by HPLC. This desorption procedure was repeated three times.

2.6. Quinclorac analysis

QC was analyzed by HPLC using an Agilent 1260 chromatogaph coupled with an Agilent UV detector. The analytical conditions used were as follows: Agilent TC-C18 column (5 μm,4.6 mm internal diameter × 250 mm length), Methanol: 1% acetid acid = 60:40 (v:v) eluent mixture at a flow rate of 1.0 mL/min, 20 μL injection volume, and UV detection at 240 nm. External calibration curves with standard QC solutions between 0.5 and 30 mg/L were used in the analyses.

3. Results and discussion

3.1. Effect of dosage of CTS in CTS–MMTS on the adsorption percentage of QC onto CTS–MMTS

Fig. 2 shows the effect of different dosage of chitosan used to prepare the composites on the adsorption percentage of QC. With the increase in dosage of chitosan (from 0 to 1.2 g), the adsorption percentage of QC significantly increases correspondingly (from 4.80 to 77.39%), since the dosage increase of CTS is helpful for balancing the initial negative charges of NaMMT and improving its adsorption capacity for anion QC [47]. However, when the dosage of CTS increased from 1.2 to 1.8 g, it resulted in only a slight increase in adsorption percentage from 77.39 to 82.81%, which has no statistical significance ($p > 0.05$). Moreover, results of the elemental analysis of the CTS–MMTS bionanocomposites in Table 1 indicated that when the dosage ratio of CTS to MMT exceeds 1.2:1, the amount of CTS loaded on the NaMMT is saturated. Based on the cost saving consideration, a dosage of 1.2 g of CTS was suitable for preparing the composite. Thereafter, the composite prepared with 1.2 g CTS and 1.0 g NaMMT (named as CTS–MMT) is used for the following experiments.

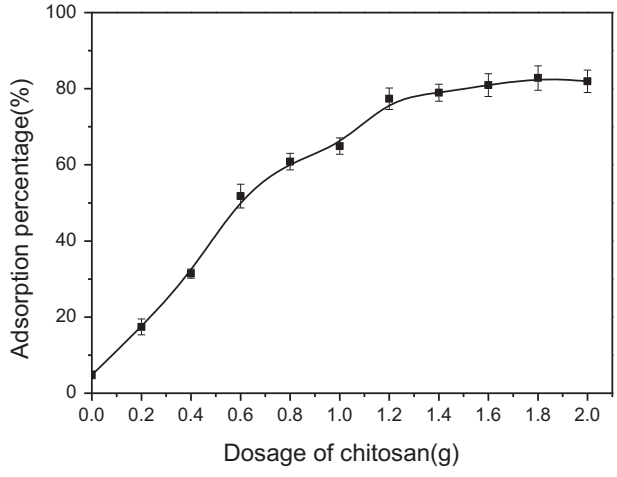

Fig. 2. Effect of dosage of CTS in CTS-MMTS on the QC adsorption.

3.2. Materials characterization

The XRD patterns of NaMMT and CTS–MMT are shown in Fig. 3. From the characteristic (0 0 1) diffraction, structural changes in the NaMMT are clearly observed. The diffraction peak (0 0 1) of NaMMT appears at 2θ of 7.14°, corresponding to the basal spacing d(0 0 1) of 1.24 nm, consistent with the presence of interlayer Na^+ retaining one layer of hydration water [43,48]. However, the d(0 0 1) basal spacing of CTS–MMT is increased from 1.24 to 1.52 nm ($2\theta = 5.82°$), indicating that one monolayer of chitosan has intercalated into the interlayers of NaMMT [43,49,50].

The nitrogen adsorption–desorption isotherms and pore diameter distributions (inset) of NaMMT and CTS–MMT are shown in Fig. 4. It can be seen in this figure that both of the two samples show a type-IV sorption isotherm with a type-H3 hysteresis loop, indicating the mesoporous structure of the materials [51]. The average pore diameters of NaMMT and CTS-MMT are 6.4 and 9.2 nm, respectively, belonging to mesopores. The specific BET surface areas of NaMMT and CTS–MMT were 69.6 and 22.8 m^2/g, respectively. The larger pore diameter and lower BET surface area of CTS–MMT are due to the packing of the CTS molecules in the internal and external surface of NaMMT, resulting in pore blocking, which impedes the passage of nitrogen [52].

The FTIR spectra of NaMMT, CTS, and CTS–MMT are shown in Fig. 5. The spectrum of CTS shows peaks at 3,433 cm^{-1} due to the overlapping of O–H and N–H stretching bands, 2,922 and 2,867 cm^{-1} for aliphatic C–H stretching vibrations, 1,657 and 1,594 cm^{-1} for N–H deformation vibrations. In the spectrum of

Table 1
Results of the elemental analysis of chitosan–montmorillonite bionanocomposites

CTS:MMT (m:m) (%)	0.0	0.2	0.4	0.6	0.8	1.0	1.2	1.4	1.6	1.8	2.0
C (%)	0.2	6.92	12.6	14.9	17.9	20.2	23.5	24.1	23.9	24.7	23.8
N (%)	–	1.33	2.25	3.01	3.73	4.12	4.58	4.57	4.59	4.56	4.57
Chitosan[a] (%)	–	15.3	25.9	34.6	42.9	47.4	52.7	52.6	52.8	52.4	52.6

[a]Calculated from the N content of the samples.

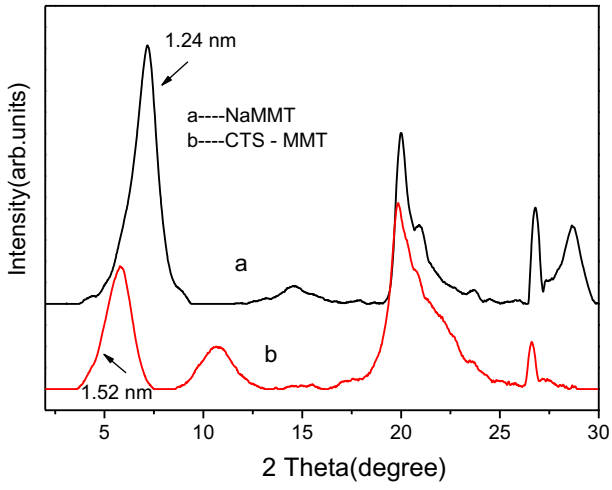

Fig. 3. X-ray diffraction patterns of NaMMT (a) and CTS–MMT (b).

NaMMT, the absorption bands at 3,629, 3,425, 1,640 cm^{-1}, corresponding to –OH stretching vibration of structural hydroxyls, –OH stretching, and bending vibrations of hydration water, are respectively identified. The spectrum of CTS–MMT shows the combination of characteristic bands of CTS and NaMMT, and these absorption bands are in agreement with the results reported for CTS–MMT composites [15,53]. Compared with the spectrum of NaMMT, the main changes of CTS–MMT spectrum are as follows: reaching peaks at 3,629, while becoming weaker at 3,425 cm^{-1}, indicating a relatively low water content, due to the replacement of the interlayer inorganic cations of NaMMT and their hydration water with CTS [43]. In addition, new peaks at about 2,930, 2,875, and 1,526 cm^{-1} represent the bending vibrations of aliphatic C–H stretching vibrations and the deformation vibration of the protonated amine group ($-NH_3^+$) [51]. It indicates that CTS has been successfully immobilized onto the NaMMT through electrostatic attraction between the $-NH_3^+$ of CTS and the negatively charged sites of NaMMT [43]. These results are in agreement with the results from XRD and BET analyses, revealing the interaction between CTS and NaMMT.

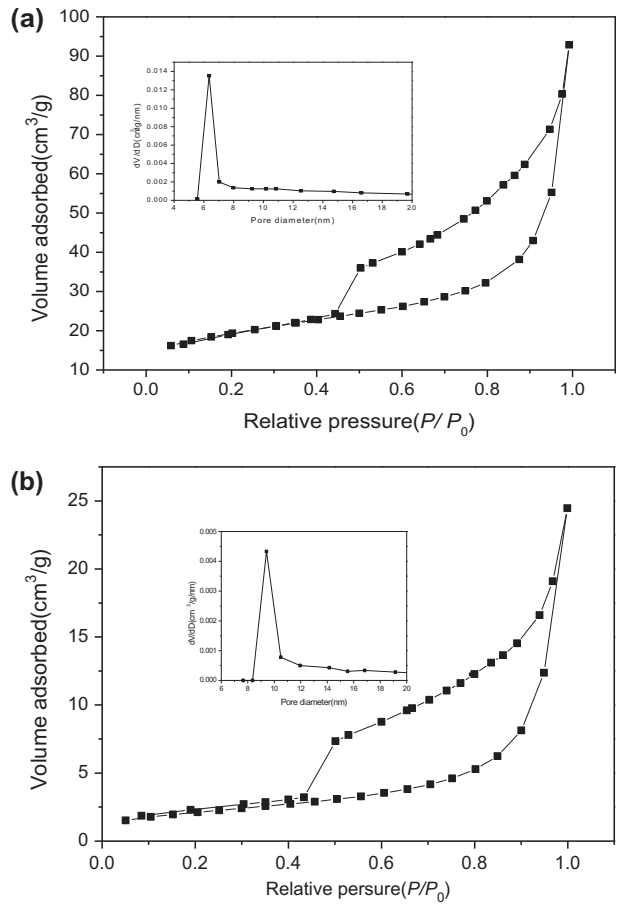

Fig. 4. Nitrogen adsorption–desorption isotherms and pore diameter distributions of NaMMT (a) and CTS–MMT (b).

Fig. 6 shows the morphologies of NaMMT (a) and CTS–MMT (b). The distinct appearance may be seen from the figure. Compared with NaMMT, the CTS–MMT has larger particles and coarse porous surface. The NaMMT particles appears to be enveloped in CTS network, probably due to the presence of CTS at both internal and external NaMMT surfaces [43]. Similar morphological images were described in previous literatures on chitosan clay composites [47,54].

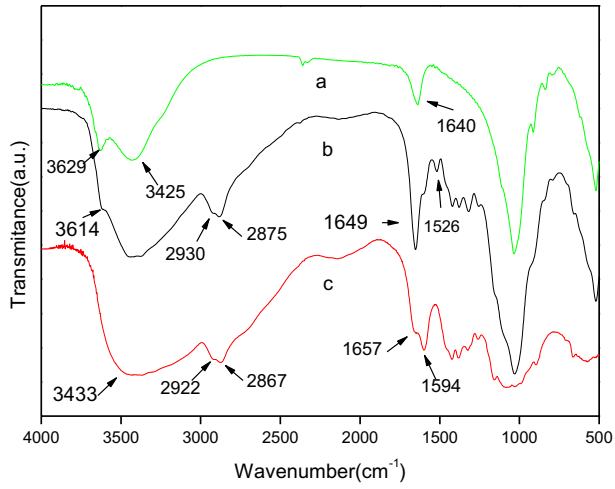

Fig. 5. FTIR spectra of NaMMT (a), CTS–MMT (b), and CTS (c).

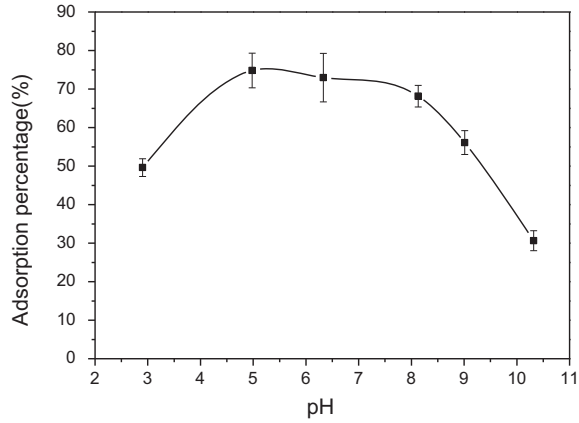

Fig. 7. Effect of pH on the adsorption of QC onto CTS–MMT.

3.3. Effect of pH on QC adsorption

The effect of initial solution pH on QC adsorption onto CTS–MMT is shown in Fig. 7. In the pH range from 2.9 to 10.3, QC adsorption percentage is relatively high at around pH 5.0–6.3 with the maximum adsorption percentage at about pH 5.0. When pH < 5.0, there is a positive correlation between the increase in adsorption of QC and the increase in pH; while when pH > 5.0, the correlation is negative. Changes in pH affected the dissociation of QC molecule and the surface charge of the CTS–MMT. According to the dissociation constant of QC ($pK_a = 4.3$), more than 50% of the QC is expected to be neutral molecular form at low pH levels ($pH < pK_a$) and the protonation degree of CTS is expected to be high, which results in the lower adsorption of QC. Weak hydrogen bonding and van der Waals interactions may be responsible for QC adsorption onto CTS–MMT at low pH. At high pH levels (e.g. pH 5.0), QC mainly exists in an anion form because of the $pH > pK_a$ and the protonation degree of CTS is above 90% [10,15], resulting in the increase of electrostatic attraction between QC and CTS–MMT. However, when adsorption occurs above pH 6.3 ($pH > pK_a$), the anionic form of QC is dominant in solution. The overall surface charge on the CTS–MMT is negative when the solution pH is greater than pH_{pzc} (6.8). In this case, the adsorption percentage of CTS–MMT for QC is reduced due to electrostatic repulsion between anionic QC and the negatively charged CTS–MMT surface.

3.4. Effect of adsorbent dosage on QC adsorption

Fig. 8 shows the effect of CTS–MMT dosage (from 1 to 20 g/L) on the QC adsorption. An increase of the amount of CTS–MMT from 1 to 10 g/L results in the rapid increase in adsorption percentage from 56.1 to 93.0%. A further increase in the CTS–MMT dosage

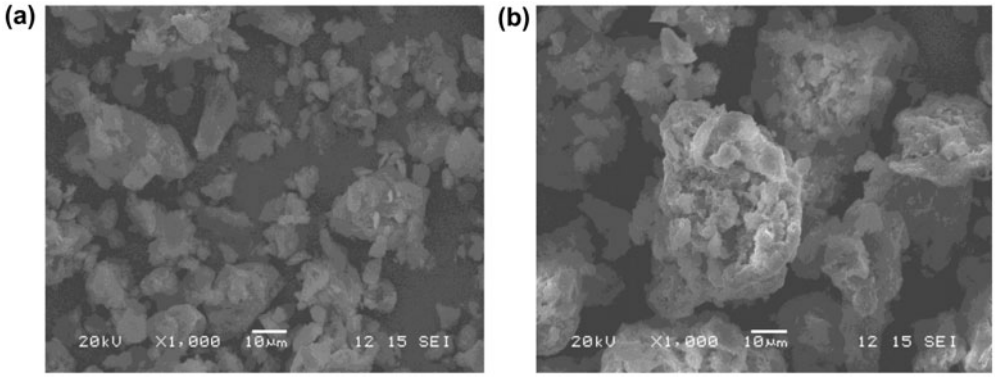

Fig. 6. SEM images of NaMMT (a) and CTS–MMT (b).

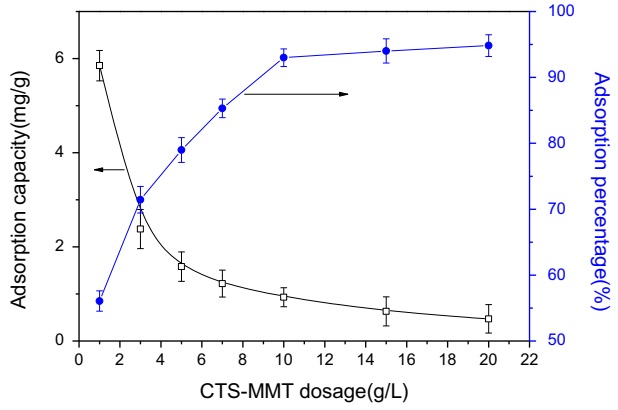

Fig. 8. Effect of CTS-MMT dosage on QC adsorption onto CTS–MMT.

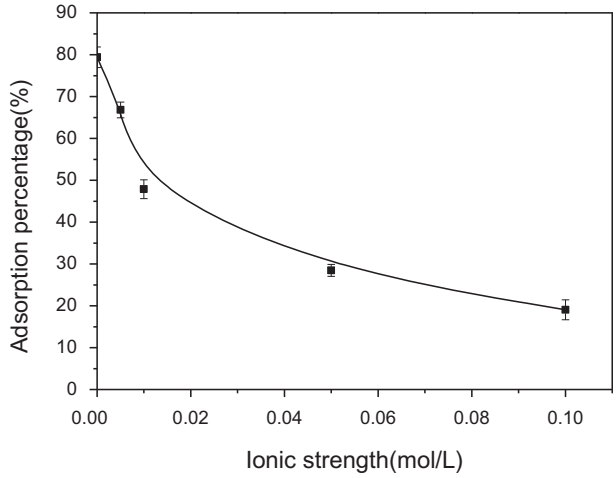

Fig. 9. Effect of ionic strength on QC adsorption onto CTS–MMT.

from 10 to 20 g/L does not lead to dramatical increase in adsorption percentage as before (only from 93.0 to 94.8%). The increase in adsorption percentage with increasing CTS–MMT dosage is attributed to the increase of adsorption active sites available for QC [32,55]. However, the QC adsorption capacity decreasing with the increasing dosage of CTS–MMT is due to adsorption active sites remaining unsaturated [32], and the concentration gradient between the QC concentration in the solution and the QC concentration in the CTS–MMT surface [55]. Based on an overall consideration, the dosage of 10 g/L is enough for the QC removal.

The effect of ionic strength on QC adsorption onto CTS–MMT at solution pH 5.1 is shown in Fig. 9. The adsorption percentage of QC reduces gradually from 79.40 to 19.07% with the increase in NaCl concentration from 0 to 0.1 mol/L, indicating that the ionic strength has a significant negative effect on the QC adsorption. The phenomenon implies that electrostatic attraction should be the main driving force between QC and CTS–MMT. The decrease in adsorption percentage in the presence of NaCl could be due to the electrostatical screening effect of salt [39,52].

3.5. Adsorption kinetics

In order to further investigate the adsorption mechanism of QC onto CTS–MMT, the pseudo-first-order equation (Eq. (3)) and pseudo-second-order equation (Eq. (4)) are used to analyze the kinetic data [56]:

$$\ln(q_e - q_t) = \ln q_e - k_1 t \tag{3}$$

$$\frac{t}{q_t} = \frac{t}{q_e} + \frac{1}{k_2 q_e^2} \tag{4}$$

where q_e and q_t are the amount of adsorbate onto adsorbent (mg/g) at equilibrium and at time t (h), respectively. k_1 (h^{-1}) is the rate constant of pseudo-first-order adsorption, the value of which is calculated from the plot of $\ln(q_e - q_t)$ vs. t. k_2 (g/(mg h)) is the rate constant of pseudo-second-order adsorption, the value of which is calculated from the plot of t/q_t vs. t.

The adsorption kinetics data of QC onto CTS–MMT are shown in Fig. 10. The adsorption of QC is fast at the beginning of the experiment but thereafter it takes about 18 h to reach equilibrium. The rate constants and theory data calculated by the kinetics equations are summarized in Table 2. As shown in Table 2, the small correlation coefficient R^2 and the large difference of adsorption capacity between the calculation and the experiment for the pseudo-first-order model indicate that pseudo-first-order model is not suitable to describe the adsorption kinetics and the adsorption is not occurring exclusively on one site [56]. However, there are very large correlation coefficient values ($R^2 = 0.999$) for the pseudo-second-order model, and the adsorption capacities calculated by the pseudo-second-order equation are in good agreement with the experimental data. Thus, the adsorption kinetics of QC onto CTS–MMT can be well described by the pseudo-second-order model, suggesting that rate-limiting step may be a chemical adsorption [22,33].

3.6. Adsorption isotherms

The adsorption isotherm of QC onto CTS–MMT is shown in Fig. 11.

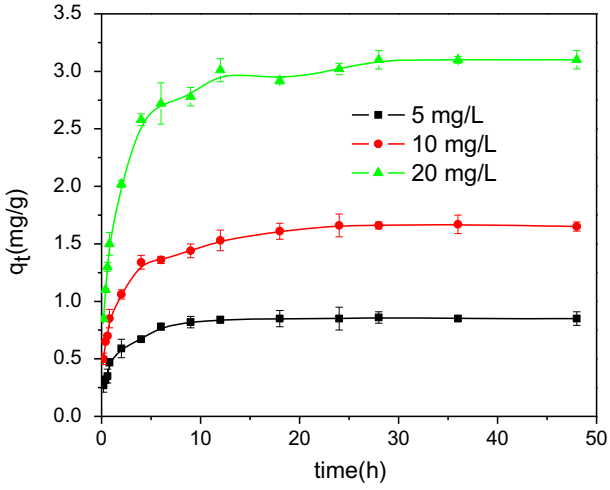

Fig. 10. Adsorption kinetics of QC onto CTS–MMT.

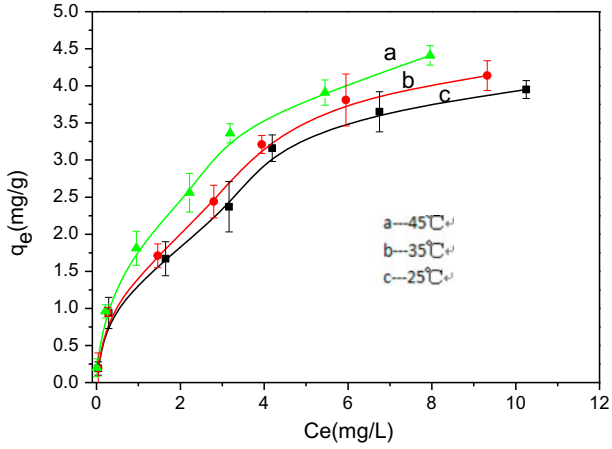

Fig. 11. Adsorption isotherm for QC adsorption onto CTS–MMT.

It shows that the QC adsorption capacity increases with the increase in QC equilibrium concentration and temperature. In order to further understand the sorption mechanism, the two most common isotherm models—Langmuir and Freundlich isotherm models are applied to fit the experimental data. The Langmuir isotherm model assumes that the adsorbent surface is homogeneous and there are no interaction forces between adsorbates [52]. The Langmuir model in its linear form can be written as follows [57]:

$$\frac{C_e}{q_e}=\frac{1}{q_m b}+\frac{C_e}{q_m} \tag{5}$$

where C_e is the concentration of QC in aqueous solution at equilibrium (mg/L), q_e is the amount of QC adsorbed at equilibrium (mg/g), q_m is the maximum adsorption capacity (mg/g), and b is the Langmuir constant (L/mg), the value of which reflects the binding strength between the adsorbate and adsorbent. The values of q_m and b can be obtained from the slope and intercept by ploting C_e/q_e vs. C_e.

The Freundlich model is an empirical equation applicable to heterogeneous adsorption [58]. The linearized form of the Freundlich equation can be written as follows:

$$\ln q_e=\ln K_F+\frac{1}{n}\ln C_e \tag{6}$$

where K_F and $1/n$ are the Freundlich empirical constants, which are related to the adsorption capacity and adsorption intensity, respectively.

The fitting parameters for QC adsorption isotherms by above two models are listed in Table 3. The fitting results show that the correlation coefficient of Freundlich equation is larger than that of Langmuir equation, indicating that the adsorption of QC onto CTS–MMT can be better fitted by Freundlich model than by Langmuir model. The values of K_F increases as the temperature increases from 298 to 318 K, suggesting stronger adsorption binding of QC onto CTS–MMT at a higher temperature. Moreover, all of the $1/n$ values are less than unity, which indicates the adsorption of QC onto CTS-MMT is favorable [52].

3.7. Adsorption thermodynamics

The effect of temperature from 15 to 35°C on the QC adsorption is investigated, and the results are shown in Fig. 11. The QC adsorption capacity increases with the increase in temperature from 15 to

Table 2
Fitting parameters of kinetic models of quinclorac adsorbed on CTS–MMT

	Pseudo-first-order equation			Pseudo-second-order equation		
$q_{e,exp}$ (mg/g)	k_1 (1/h)	$q_{e1,cal}$ (mg/g)	R^2	k_2 (g/mg h)	$q_{e2,cal}$ (mg/g)	R^2
1.66	0.0990	0.69	0.900	0.636	1.70	0.999

Table 3
Adsorption isotherm parameters for QC adsorption onto CTS–MMT

	Langmuir			Freundlich		
T (K)	b (L/mg)	q_m (mg/g)	R^2	K_F ($mg^{1-1/n}/g\ L^{1/n}$)	$1/n$	R^2
298	0.559	4.52	0.958	1.30	0.54	0.970
308	0.563	4.81	0.960	1.39	0.52	0.991
318	0.917	4.78	0.961	1.85	0.44	0.998

Table 4
Thermodynamic parameters for QC sorption onto CTS–MMT

T (K)	ΔG° (kJ/mol)	ΔH° (kJ/mol)	ΔS° (J/(mol K))	R^2
298	−16.99			
308	−18.39	24.76	140.1	0.901
318	−19.79			

35℃, indicating that the adsorption is an endothermic process.

The thermodynamic parameters such as Gibbs free energy (ΔG°), entropy (ΔS°), and enthalpy (ΔH°) are determined using the following equations [38,59]:

$$K_c = \frac{q_e}{C_e} \tag{7}$$

$$\Delta G^\circ = -RT\ \ln(1000K_c) \tag{8}$$

$$\Delta G^\circ = \Delta H^\circ - T\Delta S^\circ \tag{9}$$

$$\ln(1000\,K_c) = \frac{\Delta S^\circ}{R} - \frac{\Delta H^\circ}{RT} \tag{10}$$

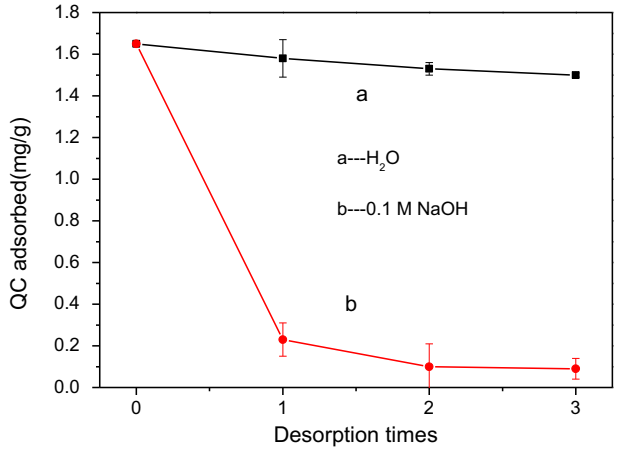

Fig. 12. QC desorption from CTS–MMT using H_2O and 0.1 M NaOH.

where K_c is the distribution coefficient of adsorbent, q_e is the amount QC adsorbed at equilibrium (mg/g), C_e is the QC concentration in the aqueous solution at equilibrium (mg/L), R is the gas constant (8.314 J/mol K), and T is the reaction temperature (K). The values of ΔS° and ΔH° are obtained from the intercept and slope of the line plotted by $\ln(1000K_c)$ against $1/T$, respectively. The obtained thermodynamic parameters are listed in Table 4. The values of ΔG° are all negative from 15 to 35℃. Moreover, the values of ΔG° become more negative as the temperature increases, indicating that the adsorption process is spontaneous and higher temperatures are more favorable for QC adsorption. The value of ΔH° is positive, implying the adsorption process is endothermic. In general, the values of ΔH° fall within the range of 2.1–20.9 kJ/mol and 80–200 kJ/mol for physical and chemical adsorption, respectively [52]. The ΔH° value of QC adsorption onto CTS–MMT is not within the range of either physical or chemical adsorption, implying that the adsorption may involve other forces such as electrostatic interaction. The positive value of ΔS° (140.1 J/mol K) suggests that the adsorption reaction is an entropy-increasing process, and there is an affinity between QC molecules and CTS–MMT surface, and that the degree of dispersion increases with the increasing temperature. [54].

3.8. Desorption studies

Desorption studies are useful in elucidating the adsorption mechanism. If the adsorbate adsorbed onto the adsorbent can be desorbed by water, it indicates that the interaction between the adsorbate and the adsorbent is by weak bonds. However, if the adsorbate can only be desorbed by strong base or acid, it suggests that the attachment of the adsorbate onto the adsorbent is by electrostatic attraction or ion exchange [31,32,60]. In this study, the desorption behavior of QC from CTS–MMT is shown in Fig. 12. The amount of desorbed QC is very small by distilled water and the percentage of desorption is only 9.09%; while in the case of 0.1 M NaOH, the high desorption

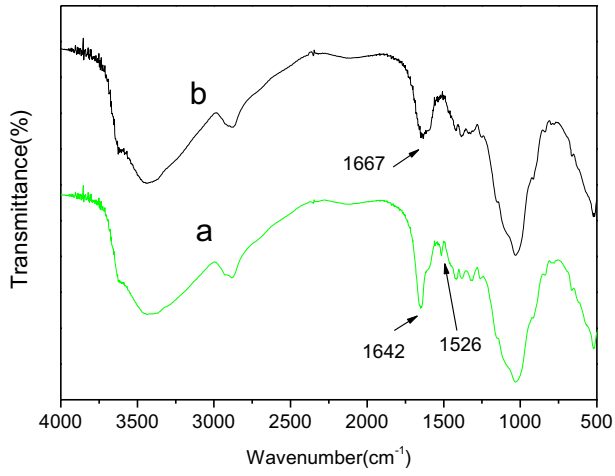

Fig. 13. FTIR spectra of CTS–MMT before (a) and after (b) adsorption QC.

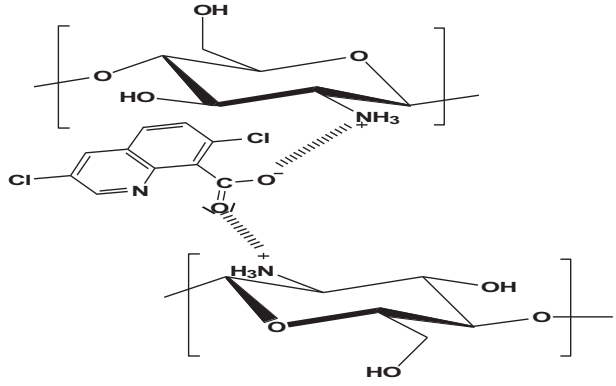

Fig. 14. Main attractions between QC and CTS–MMT.

percentage of 94.6% is obtained. This suggests that adsorption of QC onto CTS–MMT occurs mainly via electrostatic attraction [43], which is consistent with the explanation of pH effect outlined in Section 3.3.

3.9. Adsorption mechanism

Fig. 13 shows the FTIR spectra of CTS–MMT before and after adsorption of QC. Compared with the spectrum of CTS–MMT before adsorption QC, the absorption band at 1,526 cm^{-1} (the deformation vibration of $–NH_3^+$) disappears on the spectrum after adsorption, which indicates there are mainly electrostatic attraction and cation–dipole interaction between the $–NH_3^+$ and ionic QC. The peak at 1,642 cm^{-1} (–OH and N–H stretching vibration) significantly weakens and shifts to higher wavenumber after QC adsorption. This implies that –OH and $–NH_3^+$ groups are involved in the interaction between QC and CTS–MMT. The possible main attractions between QC and CTS–MMT are illustrated in Fig. 14.

4. Conclusion

In this study, CTS–MMT is synthesized and applied for the removal of QC. Characterization results show that CTS is successfully loaded on the internal and external surfaces of NaMMT, and the NaMMT modified by CTS possesses high adsorption capacity for QC. QC adsorption is strongly dependent on adsorbent dosage, pH, ionic strength, and temperature. The adsorption kinetics conform to a pseudo-second-order model and the equilibrium adsorption data fits better with the Freundlich isotherm model than the Langmuir model.

The adsorption thermodynamics suggests that higher temperatures are more favorable for QC sorption and the adsorption process is spontaneous and endothermic. The QC adsorbed on CTS–MMT can be mostly desorbed by 0.1 M NaOH but distilled water can only desorb a little amount of QC. The mechanisms for the QC adsorption may involve electrostatic attraction, cation–dipole, hydrogen bonding, and van der Waals interactions.

The results show that CTS–MMT is a promising sorbent for removing QC from aqueous solution, as previously observed for other anionic pesticides [43].

Acknowledgments

This study was supported by the National Science Foundation of China (501104064), Scientific Research Project of the Education Department of Hunan Province (13C393), the General Project of Hunan Provincial Science and Technology Department (2014sk3178), the College Students' Innovative Experiment Project of Hunan Agricultural University(XCX14087).

References

[1] K. Grossmann, Quinclorac belongs to a new class of highly selective auxin herbicides, Weed Sci. 46 (1998) 707–716.
[2] L. Pareja, A. Pérez-Parada, A. Agüera, V. Cesio, H. Heinzen, A.R. Fernández-Alba, Photolytic and photocatalytic degradation of quinclorac in ultrapure and paddy field water: Identification of transformation products and pathways, Chemosphere 87 (2012) 838–844.
[3] Z. Li, T. Shao, H. Min, Z. Lu, X. Xu, Stress response of *Burkholderia cepacia* WZ1 exposed to quinclorac and the biodegradation of quinclorac, Soil Biol. Biochem. 41 (2009) 984–990.

[4] L.A. Gettys, W.T. Haller, Response of selected foliage plants to four herbicides in irrigation water, HortTechnology 20 (2010) 921–928.
[5] A. Pretto, V.L. Loro, C. Menezes, B.S. Moraes, G.B. Reimche, R. Zanella, L.A. de Ávila, Commercial formulation containing quinclorac and metsulfuron-methyl herbicides inhibit acetylcholinesterase and induce biochemical alterations in tissues of *Leporinus obtusidens*, Ecotoxicol. Environ. Saf. 74 (2011) 336–341.
[6] J.F. Han, Z.Y. Zhang, H.S. Liu, X.Q. Wang, Progress in research in hazardous effect of residual quinclorac on flue-cured tobacco in rice fields and its restoration, Acta Tabacaria Sin. 19 (2013) 81–83.
[7] C. Resgalla Jr., J.A. Noldin, M.S. Tamanaha, F.C. Deschamps, D.S. Eberhardt, L.R. Rörig, Risk analysis of herbicide quinclorac residues in irrigated rice areas, Santa Catarina, Brazil, Ecotoxicology 16 (2007) 565–571.
[8] P.J. Rice, P.J. Rice, E.L. Arthur, A.C. Barefoot, Advances in pesticide environmental fate and exposure assessments, J. Agric. Food Chem. 55 (2007) 5367–5376.
[9] S. Sauco, G. Eguren, H. Heinzen, O. Defeo, Effects of herbicides and freshwater discharge on water chemistry, toxicity and benthos in a Uruguayan sandy beach, Mar. Environ. Res. 70 (2010) 300–307.
[10] A. Pusino, A. Gelsomino, M.G. Fiori, C. Gessa, Adsorption of two quinolinecarboxylic acid herbicides on homoionic montmorillonites, Clays Clay Miner. 51 (2003) 143–149.
[11] J.D. Mattice, B.W. Skulman, R.J. Norman, E.E. Gbur, , Analysis of river water for rice pesticides in eastern Arkansas from 2002 to 2008, J. Soil Water Conserv. 65 (2010) 130–140.
[12] M.V. Pinna, A. Pusino, Direct and indirect photolysis of two quinolinecarboxylic herbicides in aqueous systems, Chemosphere 86 (2012) 655–658.
[13] J.Y. Dong, K. Luo, L.Y. Bai, X.M. Zhou, A.P. Zeng, J. Fan, Isolation, identification, identification and characterization of an Alcaligenes strain capable of degrading quinclorac, Chin. J. Pestic. Sci. 15 (2013) 316–322.
[14] C.X. Ding, Z.J. He, C. Zheng, L.M. Cai, D.X. Gong, Studies of quinclorac adsorption on HDTMAB modified montmorillonite, J. Agro-Environ. Sci. 33 (2014) 1755–1761.
[15] Y.H. Deng, L. Wang, X.B. Hu, B.Z. Liu, Z.B. Wei, S.G. Yang, C. Sun, Highly efficient removal of tannic acid from aqueous solution by chitosan-coated attapulgite, Chem. Eng. J. 181–182 (2012) 300–306.
[16] O. Abollino, M. Aceto, M. Malandrino, C. Sarzanini, E. Mentasti, Adsorption of heavy metals on Na-montmorillonite. Effect of pH and organic substances, Water Res. 37 (2003) 1619–1627.
[17] G.A. Khoury, T.C. Gehris, L. Tribe, R.M.T. Sánchez, M. dos Santos Afonso, Glyphosate adsorption on montmorillonite: An experimental and theoretical study of surface complexes, Appl. Clay Sci. 50 (2010) 167–175.
[18] C.J. Wang, Z. Li, W.T. Jiang, J.S. Jean, C.C. Liu, Cation exchange interaction between antibiotic ciprofloxacin and montmorillonite, J. Hazard. Mater. 183 (2010) 309–314.
[19] Q. Wu, Z. Li, H. Hong, K. Yin, L. Tie, Adsorption and intercalation of ciprofloxacin on montmorillonite, Appl. Clay Sci. 50 (2010) 204–211.
[20] A.H. Gemeay, A.S. El-Sherbiny, A.B. Zaki, Adsorption and kinetic studies of the intercalation of some organic compounds onto Na^+-montmorillonite, J. Colloid Interface Sci. 245 (2002) 116–125.
[21] R. Ganigar, G. Rytwo, Y. Gonen, A. Radian, Y.G. Mishael, Polymer–clay nanocomposites for the removal of trichlorophenol and trinitrophenol from water, Appl. Clay Sci. 49 (2010) 311–316.
[22] M. Mekhloufi, A. Zehhaf, A. Benyoucef, C. Quijada, E. Morallon, Removal of 8-quinolinecarboxylic acid pesticide from aqueous solution by adsorption on activated montmorillonites, Environ. Monit. Assess. 185 (2013) 10365–10375.
[23] D. Kovacević, J. Lemić, M. Damjanović, R. Petronijević, Đ. Janaćković, T. Stanić, Fenitrothion adsorption–desorption on organo-minerals, Appl. Clay Sci. 52 (2011) 109–114.
[24] M.J. Sanchez-Martin, M.S. Rodriguez-Cruz, M.S. Andrades, M. Sanchez-Camazano, Efficiency of different clay minerals modified with a cationic surfactant in the adsorption of pesticides: Influence of clay type and pesticide hydrophobicity, Appl. Clay Sci. 31 (2006) 216–228.
[25] M.J. Sánchez-Martín, M.C. Dorado, C. del Hoyo, M.S. Rodríguez-Cruz, Influence of clay mineral structure and surfactant nature on the adsorption capacity of surfactants by clays, J. Hazard. Mater. 150 (2008) 115–123.
[26] D. Zadaka, S. Nir, A. Radian, Y.G. Mishael, Atrazine removal from water by polycation–clay composites: Effect of dissolved organic matter and comparison to activated carbon, Water Res. 43 (2009) 677–683.
[27] A. Radian, Y.G. Mishael, Characterizing and designing polycation–clay nanocomposites as a basis for imazapyr controlled release formulations, Environ. Sci. Technol. 42 (2008) 1511–1516.
[28] A. Radian, Y. Mishael, Effect of humic acid on pyrene removal from water by polycation-clay mineral composites and activated carbon, Environ. Sci. Technol. 46 (2012) 6228–6235.
[29] M. Cruz-Guzmán, R. Celis, M.C. Hermosín, J. Cornejo, Adsorption of the herbicide simazine by montmorillonite modified with natural organic cations, Environ. Sci. Technol. 38 (2004) 180–186.
[30] M.Y. Chang, R.S. Juang, Adsorption of tannic acid, humic acid, and dyes from water using the composite of chitosan and activated clay, J. Colloid Interface Sci. 278 (2004) 18–25.
[31] L. Wang, J. Zhang, A. Wang, Fast removal of methylene blue from aqueous solution by adsorption onto chitosan-g-poly (acrylic acid)/attapulgite composite, Desalination 266 (2011) 33–39.
[32] Y. Peng, D. Chen, J. Ji, Y. Kong, H. Wan, C. Yao, Chitosan-modified palygorskite: Preparation, characterization and reactive dye removal, Appl. Clay Sci. 74 (2013) 81–86.
[33] W. Ngah, W. Saime, N.F.M. Ariff, A. Hashim, M.A.K.M. Hanafiah, Malachite green adsorption onto chitosan coated bentonite beads: Isotherms, kinetics and mechanism, Clean—Soil, Air, Water 38 (2010) 394–400.

[34] S. Kittinaovarat, P. Kansomwan, N. Jiratumnukul, Chitosan/modified montmorillonite beads and adsorption Reactive Red 120, Appl. Clay Sci. 48 (2010) 87–91.
[35] B. Liu, D. Wang, G. Yu, X. Meng, Adsorption of heavy metal ions, dyes and proteins by chitosan composites and derivatives—A review, J. Ocean Univ. China 12 (2013) 500–508.
[36] V. Nair, A. Panigrahy, R. Vinu, Development of novel chitosan-lignin composites for adsorption of dyes and metal ions from wastewater, Chem. Eng. J. 254 (2014) 491–502.
[37] R. Darvishi Cheshmeh Soltani, A.R. Khataee, M. Safari, S.W. Joo, Preparation of bio-silica/chitosan nanocomposite for adsorption of a textile dye in aqueous solutions, Int. Biodeterior. Biodegrad. 85 (2013) 383–391.
[38] C.M. Futalan, C.C. Kan, M.L. Dalida, K.J. Hsien, C. Pascua, M.W. Wan, Comparative and competitive adsorption of copper, lead, and nickel using chitosan immobilized on bentonite, Carbohydr. Polym. 83 (2011) 528–536.
[39] Q. Gao, H. Zhu, W.J. Luo, S. Wang, C.G. Zhou, Preparation, characterization, and adsorption evaluation of chitosan-functionalized mesoporous composites, Microporous Mesoporous Mater. 193 (2014) 15–26.
[40] W.S. Wan Ngah, L.C. Teong, R.H. Toh, M.A.K.M. Hanafiah, Comparative study on adsorption and desorption of Cu(II) ions by three types of chitosan–zeolite composites, Chem. Eng. J. 223 (2013) 231–238.
[41] J.H. An, S. Dultz, Adsorption of tannic acid on chitosan-montmorillonite as a function of pH and surface charge properties, Appl. Clay Sci. 36 (2007) 256–264.
[42] M. Darder, M. Colilla, E. Ruiz-Hitzky, Biopolymer–clay nanocomposites based on chitosan intercalated in montmorillonite, Chem. Mater. 15 (2003) 3774–3780.
[43] R. Celis, M.A. Adelino, M.C. Hermosín, J. Cornejo, Montmorillonite–chitosan bionanocomposites as adsorbents of the herbicide clopyralid in aqueous solution and soil/water suspensions, J. Hazard. Mater. 209–210 (2012) 67–76.
[44] X.L. Han, China's Agricultural Encyclopedia (Pesticide), China Agriculture Press, Beijing, 1993, pp. 76–77 (in China).
[45] A.S.K. Kumar, S. Kalidhasan, V. Rajesh, N. Rajesh, Microwave assisted preparation and characterization of biopolymer-clay composite material and its application for chromium detoxification from industrial effluent, Adv. Mater. Lett. 2 (2011) 383–391.
[46] Y. Zhou, X.Y. Jin, H. Lin, Z.L. Chen, Synthesis, characterization and potential application of organobentonite in removing 2,4-DCP from industrial wastewater, Chem. Eng. J. 166 (2011) 176–183.
[47] L. Wang, A.Q. Wang, Adsorption characteristics of Congo Red onto the chitosan/montmorillonite nanocomposite, J. Hazard. Mater. 147 (2007) 979–985.
[48] H.J. Nam, T. Ebina, F. Mizukami, Formability and properties of self-standing clay film by montmorillonite with different interlayer cations, Colloids Surf., A 346 (2009) 158–163.
[49] H. Wang, H. Tang, Z. Liu, X. Zhang, Z. Hao, Z. Liu, Removal of cobalt(II) ion from aqueous solution by chitosan–montmorillonite, J. Environ. Sci. 26 (2014) 1879–1884.
[50] Y.S. Han, S.H. Lee, K.H. Choi, I. Park, Preparation and characterization of chitosan–clay nanocomposites with antimicrobial activity, J. Phys. Chem. Solids 71 (2010) 464–467.
[51] P. Monvisade, P. Siriphannon, Chitosan intercalated montmorillonite: Preparation, characterization and cationic dye adsorption, Appl. Clay Sci. 42 (2009) 427–431.
[52] J. Lin, Y. Zhan, Adsorption of humic acid from aqueous solution onto unmodified and surfactant-modified chitosan/zeolite composites, Chem. Eng. J. 200–202 (2012) 202–213.
[53] L. Wang, A.Q. Wang, Adsorption behaviors of Congo red on the N,O-carboxymethyl-chitosan/montmorillonite nanocomposite, Chem. Eng. J. 143 (2008) 43–50.
[54] M. Auta, B.H. Hameed, Chitosan–clay composite as highly effective and low-cost adsorbent for batch and fixed-bed adsorption of methylene blue, Chem. Eng. J. 237 (2014) 352–361.
[55] H.Y. Zhu, R. Jiang, L. Xiao, Adsorption of an anionic azo dye by chitosan/kaolin/γ-Fe_2O_3 composites, Appl. Clay Sci. 48 (2010) 522–526.
[56] X. Zou, J. Pan, H. Ou, X. Wang, W. Guan, C. Li, Y. Yan, Adsorptive removal of Cr(III) and Fe(III) from aqueous solution by chitosan/attapulgite composites: Equilibrium, thermodynamics and kinetics, Chem. Eng. J. 167 (2011) 112–121.
[57] H. El Harmoudi, L. El Gaini, E. Daoudi, M. Rhazi, Y. Boughaleb, M.A. El Mhammedi, A. Migalska-Zalas, Removal of 2,4-D from aqueous solutions by adsorption processes using two biopolymers: Chitin and chitosan and their optical properties, Opt. Mater. 36 (2014) 1471–1477.
[58] C. Umpuch, S. Sakaew, Adsorption characteristics of reactive black 5 onto chitosan-intercalated montmorillonite, Desalin. Water Treat. 53 (2015) 2962–2969.
[59] D. Chen, W. Li, Y. Wu, Q. Zhu, Z. Lu, G. Du, Preparation and characterization of chitosan/montmorillonite magnetic microspheres and its application for the removal of Cr(VI), Chem. Eng. J. 221 (2013) 8–15.
[60] Y. Zheng, J. Zhang, A. Wang, Fast removal of ammonium nitrogen from aqueous solution using chitosan-g-poly (acrylic acid)/attapulgite composite, Chem. Eng. J. 155 (2009) 215–222.